

Computations of Compound Droplet Formation in a Flow Focusing Device

***S. Homma**

Division of Materials Science, Graduate School of Science and Engineering, Saitama University,
255 Shimo-Okubo, Sakura-ku, Saitama 338-8570, Japan

*Corresponding author: honma@apc.saitama-u.ac.jp

Abstract

The formation of compound droplets in a flow focusing device is simulated numerically by a three-fluid front-tracking method. The geometry of the device and the flow rates of core, shell, and external fluids are changed to examine the effects of those on the formation of compound droplets. Several modes of the formation were observed: simple droplets (no core droplets) formation, regular compound droplets formation in jetting and dripping. They are mapped on the diagram of non-dimensional numbers, the viscosity ratio and the Capillary number. It was observed that the size of the compound droplets abruptly increased as the flow rate of the shell fluid was increased. It suggests that the mode changes suddenly due to the balance of the flow rates among core, shell, and external fluids.

Keywords: Compound droplets, Front-tracking, Flow focusing device

Introduction

Compound droplets, which consist of two immiscible phases (core and shell) in yet another immiscible continuous phase, have attracted considerable attention, because of its potential to manufacture highly structural materials such as micro capsules for drug delivery vehicle (Prankerd and Stella, 1990). If mono-dispersed compound droplets are obtained without any separation or classification, high-quality products are yielded inexpensively.

Utada *et al.* (2005) successfully fabricated mono-dispersed tiny compound droplets using the micro-fluidic device, which had co-axial dual nozzle with an outlet of an external flow outside of the nozzle. They controlled the flow of external fluid to form a thin compound jet breaking up at the tip, where tiny compound droplets are produced. This is the so-called flow focusing device, where strong external flow through a constriction draws a thin jet of the second immiscible liquid from the nozzle. Even though they have experimentally quantified to determine the size of the resulting droplets, full examination in large parameter space including physical properties and flow ratios, has not been done yet.

Homma *et al.* (2013) carried out numerical simulations for a flow focusing device by changing flow rates and physical properties. They obtained several modes of compound droplet formation and the modes were mapped on the diagram of non-dimensional numbers, as done by Zhou *et al.* (2006). In this paper, we will review this work and show recent results changing the flow rate of a shell fluid.

Problem Definition and Numerical Methods

Figure 1 shows a schematic of the problem, formation of compound droplets by a flow focusing device. In the flow focusing device, core and shell fluids of compound droplets are injected from an inner nozzle of R_{co} and an outer one of R_{sh} , respectively. An external flow is imposed to enhance the droplet formation. The radius of the cylindrical tube is R_{out} . The length and the thickness of the nozzles are L_0 and R_{th} , respectively. In order to focus the external flow toward the core and shell fluids, an obstacle is set apart from the nozzle exit. The radius of the hole of the obstacle is $R_{orifice}$ and the thickness of the obstacle is L_2 .

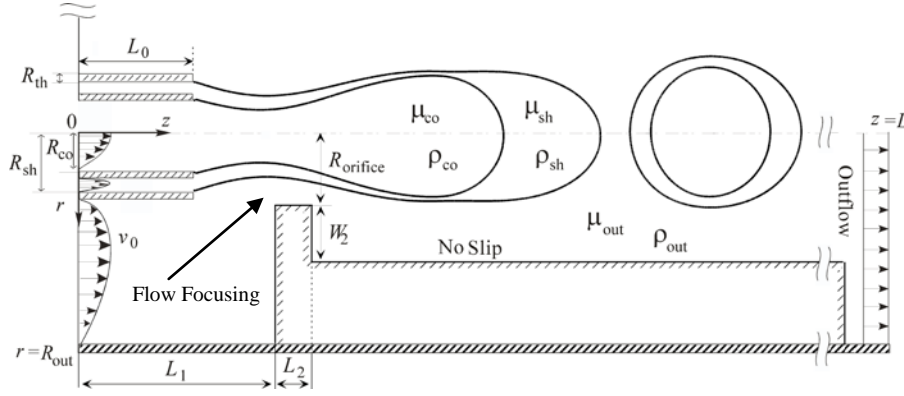


Figure 1. Schematic diagram of the simulation of compound droplet formation by flow focusing device

All three fluids are assumed to be Newtonian, incompressible, and immiscible. When this situation is described with one fluid model, the governing equations are as follows:

$$\nabla \cdot \mathbf{u} = 0, \quad (1)$$

$$\frac{\partial}{\partial t} \rho \mathbf{u} + \nabla \cdot \rho \mathbf{u} \mathbf{u} = -\nabla P + \nabla \cdot \mu (\nabla \mathbf{u} + \nabla \mathbf{u}^T) + \int_f \sigma \kappa \mathbf{n}_f \delta(\mathbf{x} - \mathbf{x}_f) dA_f, \quad (2)$$

$$\frac{D}{Dt} \rho = \frac{D}{Dt} \mu = 0, \quad (3)$$

Here, \mathbf{u} is the velocity vector and P the pressure. The surface tension is found using twice the mean curvature, κ , the unit normal of the interface, \mathbf{n}_f , and a delta function, $\delta(\mathbf{x} - \mathbf{x}_f)$, which is zero everywhere except at the interface, \mathbf{x}_f .

Eqs. (1) and (2) are discretized on the axisymmetric cylindrical coordinate by finite difference approximations with second order. The boundary conditions of z -axis are symmetry, and those of the tube wall ($r = R_{out}$) are no-slip. The boundary conditions of the exit of the tube are out flow. At the inlet of the tube, inflow boundary conditions, which are fully developed velocity distributions for cylinders and annular pipes, are applied as follows (Bird *et al.*, 2006):

$$v_0(r) = 2v_{0,co} \left[1 - \left(\frac{r}{R_{co}} \right)^2 \right] \quad \text{at } 0 \leq r \leq R_{co}, \quad (4)$$

$$v_0(r) = 2v_{0,sh} \left[\frac{\ln(1/\alpha)}{\ln(1/\alpha) \cdot (1 + \alpha^2) - (1 - \alpha^2)} \right] \left[1 - \left(\frac{r}{R_{sh}} \right)^2 - \frac{1 - \alpha^2}{\ln(1/\alpha)} \cdot \ln \left(\frac{R_{sh}}{r} \right) \right] \quad \text{at } R_{co} + R_{th} \leq r \leq R_{sh}, \quad (5)$$

$$v_0(r) = 2v_{0,out} \left[\frac{\ln(1/\gamma)}{\ln(1/\gamma) \cdot (1 + \gamma^2) - (1 - \gamma^2)} \right] \left[1 - \left(\frac{r}{R_{out}} \right)^2 - \frac{1 - \gamma^2}{\ln(1/\gamma)} \cdot \ln \left(\frac{R_{out}}{r} \right) \right] \quad \text{at } R_{sh} + R_{th} \leq r \leq R_{out}. \quad (6)$$

Here, $\alpha = (R_{co} + R_{th})/R_{out}$ and $\gamma = (R_{sh} + R_{th})/R_{out}$. The symbols $v_{0,co}$, $v_{0,sh}$, and $v_{0,out}$ are the average injection velocities for core, shell, and external fluids, respectively.

The motion of interfaces was traced by a front-tracking method (Unverdi and Tryggvason, 1992). The detailed description of the front-tracking method was given by Tryggvason *et al.* (2001) and an axisymmetric version for jet breakup into droplets was explained by Homma, *et al.* (2006 and 2010). The extension of the front-tracking method for three-fluid was described by Homma, *et al.* (2011) and its validation for compound jets and droplets was found in Vu *et al.* (2012).

Results and Discussion

The geometries of the flow focusing device were set based on the numerical study by Zhou *et al.* (2006). The sizes have been normalized by the inner radius of the outer nozzle R_{sh} and fixed as follows: $R_{co}/R_{sh} = 0.6$, $R_{out}/R_{sh} = 1.6$, $R_{th}/R_{sh} = 0.08$, $L/R_{sh} = 19.6$, $L_0/R_{sh} = 1.0$, $L_1/R_{sh} = 2.2$, $L_2/R_{sh} = 0.4$, $R_{orifice}/R_{sh} = 0.4$, and $W_2/R_{sh} = 0.4$. In order to increase accuracy, denser grid meshes in r direction were arranged near the dual nozzle. By preliminary grid refinement tests, the grid resolution was determined as 128x2048.

Physical properties were set referring to the study by Utada *et al.* (2005) and Zhou *et al.* (2006). Density ratios were fixed as follows: $\rho_{sh}/\rho_{co} = 1.25$ and $\rho_{out}/\rho_{co} = 1.22$. The viscosity ratio between core and shell fluids (μ_{sh}/μ_{co}) was fixed at unity. The viscosity ratio between core and ambient fluids was changed as a parameter ($\beta = \mu_{out}/\mu_{co}$). Interfacial tension coefficient between core and shell fluids and that between shell and ambient fluids were set to be the same.

The definition of non-dimensional numbers and their ranges are as follows: $Re_{co} = D_{co}v_{0,co}\rho_{co}/\mu_{co}$ ($9.72 \times 10^{-3} < Re_{co} < 1.18$), $Re_{sh} = D_{sh}v_{0,sh}\rho_{sh}/\mu_{sh}$ ($1.06 \times 10^{-2} < Re_{sh} < 0.960$), $Re_{out} = D_{out}v_{0,out}\rho_{out}/\mu_{out}$ ($9.17 \times 10^{-3} < Re_{out} < 36.7$), $We_{co} = D_{co}v_{0,co}^2\rho_{co}/\sigma$ ($1.18 \times 10^{-4} < We_{co} < 1.18 \times 10^{-2}$), $We_{sh} = D_{sh}v_{0,sh}^2\rho_{sh}/\sigma$ ($6.40 \times 10^{-5} < We_{sh} < 8.47 \times 10^{-3}$), $We_{out} = D_{out}v_{0,out}^2\rho_{out}/\sigma$ ($1.33 \times 10^{-3} < We_{out} < 4.89 \times 10^{-1}$), and $Ca_{co} = We_{co}/Re_{co}$, where D is the hydraulic diameter defined by $D_{co} = 2R_{co}$, $D_{sh} = 2(R_{sh}-R_{th}-R_{co})$, or $D_{out} = 2(R_{out}-R_{th}-R_{sh})$. The viscosity ratio β was chosen one from among 0.1, 0.5, 1, 5, and 10.

Figure 2 shows instantaneous interfacial shapes for three different cases ($\beta = 1$). In case (a), uniform compound droplets are successfully produced in a fairly regular manner. This is a dripping mode (Homma, *et al.*, 2006 and 2010) and the orifice acts as a nozzle. In case (b), only We_{out} is different (1.33×10^{-1}) from case (a), where the external flow is much faster than that of case (a). A compound jet is produced and breaks up into compound droplets. This is a typical jetting mode (Homma, *et al.*, 2006 and 2010). The external flow accelerates at the orifice and the dispersed core and shell fluids are dragged by the external flow and a compound jet forms. Capillary waves are growing on the jet surface and compound droplets break off. In case (c), just one compound droplet is observed in the middle of the domain. All others are simple droplets of shell fluid. In this case, the supply of core fluid is not sufficient and no-core simple droplets are mainly produced.

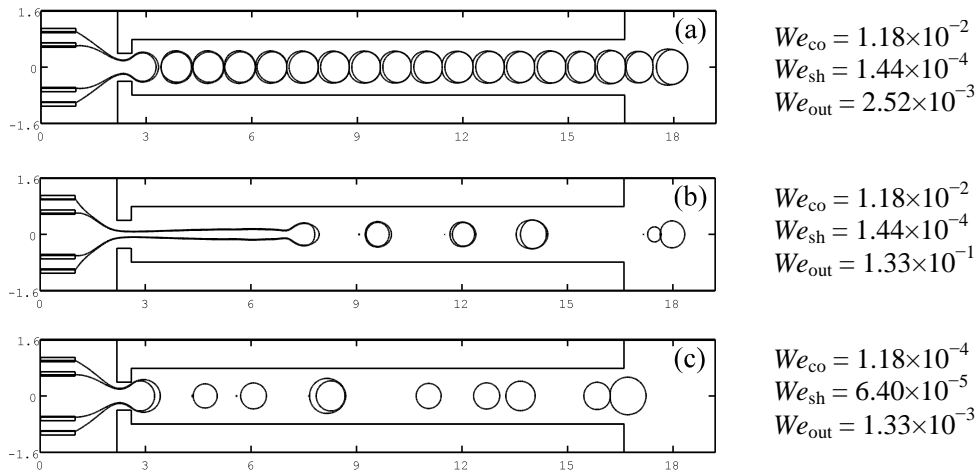


Figure 2. Instantaneous shapes of jets and droplets

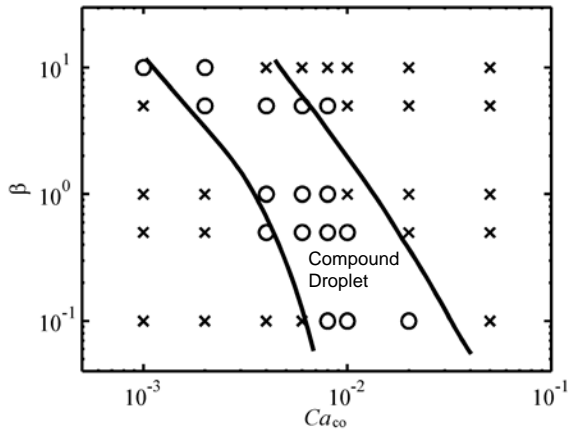


Figure 3. Map of compound droplet formation ($We_{co} = 3.89 \times 10^{-4}$); ○: successful formation, ×: unsuccessful formation

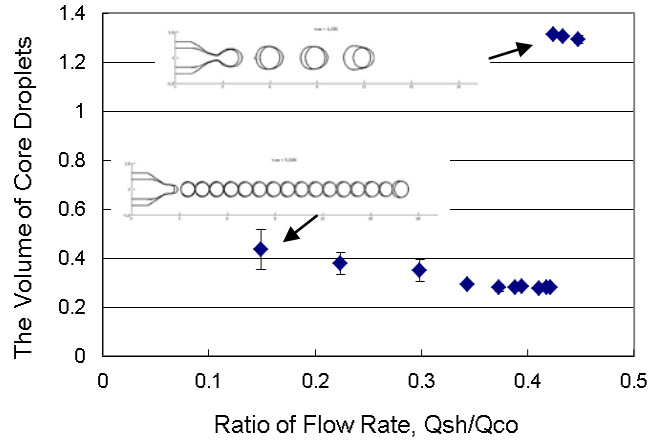


Figure 4. Volume of core droplet vs. ratio of flow rate between core and shell fluids

Figure 3 shows a map of compound droplet formation on the diagram of β vs. Ca_{co} for $We_{co} = 3.89 \times 10^{-4}$. This map is identical with Fig. 16 of Zhou *et al.* (2006). All plots are obtained from our computations and the solid lines are the border between success and failure of compound droplet formation determined by Zhou *et al.* (2006). The range of the success formation of compound droplets is almost exactly the same between Zhou *et al.* (2006) and this study.

Figure 4 shows the relationship between the volume of core droplet and the ratio of the flow rate between core and shell fluids. The viscosity ratio β is 1. As the ratio of the flow rate increases, where the flow rate of the shell fluid increases, the volume of core droplets as well as compound droplet itself slightly decreases. Around the ratio 4.2, however, the volume of core droplet abruptly increases. Embedded figures show instantaneous shapes of jet and droplets. The droplets observed after the critical ratio were about 4 times larger before the critical one. It suggests that the increasing flow of the shell fluid slows the growth of capillary waves at the interface between core and shell fluids and a series of 4 waves may become one compound droplet. The similar phenomenon was observed in other viscosity ratio but the critical flow rate is different. Although the detailed investigation is underway, the flow rate of shell fluid can be one of the control parameters for the size of compound droplets.

Conclusions

The formation of compound droplets in a flow focusing device is simulated numerically by a three-fluid front-tracking method. The modes of droplet formation, simple droplets with no core and compound droplets were observed and they were mapped on the diagram, the viscosity ratio vs. Capillary number in terms of core fluid. The volume of core droplet as well as compound droplet itself suddenly increases as the flow rate of shell fluid increases beyond a critical value. The flow rate of shell fluid can be one of the control parameters for the size of compound droplets.

Acknowledgement

I am grateful to Professor Gretar Tryggvason for providing an original front-tracking code, and Professor Jiro Koga for useful discussion of this problem. I want to thank Mr. Kouta Moriguchi and Mr. Taeseon Kim for their assistance in computations. This research is supported in part by Japan Society for the Promotion of Science, Grant-in-Aid for Scientific Research (C) 24560917.

References

- Bird, R. B., Stewart, W. E. and Lightfoot, E. N. (2006), *Transport Phenomena*, 2nd Ed., John Wiley & Sons, New York, U.S.A.
- Homma, S., Koga, J., Matsumoto, S., Song, M. and Tryggvason, G. (2006), Breakup mode of an axisymmetric liquid jet injected into another immiscible liquid, *Chemical Engineering Science*, 61, pp. 3986–3996.
- Homma, S., Yokotsuka, M. and Koga, J. (2010), Numerical simulation of the formation of jets and drops in co-flowing ambient fluid, *Journal of Chemical Engineering of Japan*, 43, pp. 7–12.
- Homma, S., Yokotsuka, M., Tanaka, T., Moriguchi, K., Koga, J. and Tryggvason, G. (2011), Numerical simulation of a compound droplet by three-fluid front-tracking method,” *Fluid Dynamics & Materials Processing*, 7, 231–240.
- Homma, S., Moriguchi, K., Kim, T. and Koga, J. (2013), Computations of compound droplet formation from a co-axial dual nozzle by three-fluid front tracking method, *Journal of Chemical Engineering of Japan*, in press.
- Pranker, R. J. and Stella, V. J. (1990), The use of oil-in-water emulsions as a vehicle for parenteral drug administration,” *J. Parenteral Sci. Technol.*, 44, pp. 139–149.
- Vu, T. V., Homma, S., Tryggvason, G., Wells, J. C. and Takakura, H. (2012), Computations of breakup modes in laminar compound liquid jets in a coflowing fluid, *International Journal of Multiphase Flow*, 49, pp. 58–69.
- Tryggvason, G., Bunner, B., Esmaeeli, A., Juric, D., Al-Rawahi, N., Tauber, T., Han, J., Nas, S. and Jan, Y. (2001), A front-tracking method for the computations of multiphase flow,” *Journal of Computational Physics*, 169, pp. 708–759.
- Unverdi, S. O. and Tryggvason, G. (1992), A front tracking method for viscous, incompressible, multi-fluid flows, *Journal of Computational Physics*, 100, pp. 25–37.
- Utada, A. S., Lorenceau, E., Link, D. R., Kaplan, P. D., Stone, H. A. and Weitz, D. A. (2005), Monodispersed double emulsions generated from a microcapillary device, *Science*, 308, pp. 537–541.
- Zhou, C., Yue, P. and Feng, J. J. (2006), Formation of simple and compound drops in microfluidic devices, *Physics of Fluids*, 18, 092105–092105–14.